Japan Society of Civil Engineers 2023 Annual Meeting

# Nonlinear FE analysis for cyclic loading tests of RC pier model with measures to improve toughness

Kyushu University Student member ○Wang Wenming
Kyushu University Regular member Hiroki Tamai
Kyushu University Fellow member Yoshimi Sonoda
Nippon Koei Co.,Ltd Fellow member Masami Koshiishi

## 1. INTRODUCTION

To improve the seismic performance of reinforced concrete (RC) pier, it is necessary to give sufficient consideration not only to the strength but also to the toughness. Many researchers studied on the methods and materials for enhancing the toughness of RC pier such using transverse reinforcement in the form of closed hoop or ties (T. Y. Yuen 2017) and steel jacketing (D. Zhang 2020), fiber-reinforced plastics (FRP) (R.M.Faysal 2023), Velcro seismic reinforcement system (VSRS) (S.Kim 2022). In our other study, a new toughness improving measure for RC piers was proposed by using axial reinforcing bars with a preformed inward bending at the plastic hinges as Fig.1 shown. In this paper, to do parameters analysis, the normal RC pier and one building by proposed method were conducted by cyclic lateral loading numerical simulations in DIANA. The simulation was validated against the experiment results that were published in the companion's article by hysteretic curves and crack pattern at the peak load point.

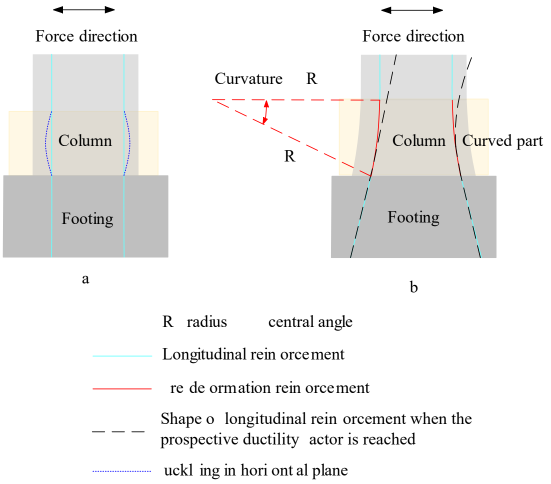


Fig. 1: the comparison of the design philosophy between normal specimen and proposed toughness improvement specimen (a) Normal specimen (b) Specimen proposed toughness improvement

## 2. Overview of the finite element model

FEM model of piers were shown in Fig.2. The loading device, cap, and footing were modeled using twenty-node structural solid. Out of simplified, the mechanical part of loading device was modelled by elastic rigid steel body. Fig.3 show the dimensions and reinforcement details of two types.

The longitudinal reinforcements and stirrup were modelled by truss bond-slip bar. However, other steel bar in cap and footing were embedded inside the concrete elements. Two yellow surfaces of footing were absolutely constrained in XYZ directions for type 1 and type 2, as the Fig.2 shown. Meanwhile, load controller and cap were only fixed at Z direction, as the Fig2. The models were subjected to two stages of applied forces. Firstly, the constant axial compressive loads were added on the face of loading controller in X direction. Then the cyclic lateral load controlled by displacements were applied in Y direction on one edge of loading controller, as Fig.2 shown.

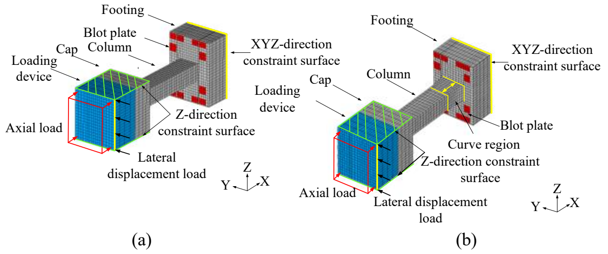


Fig. 2: FEM model of specimens (a) Type 1(b) Type 2

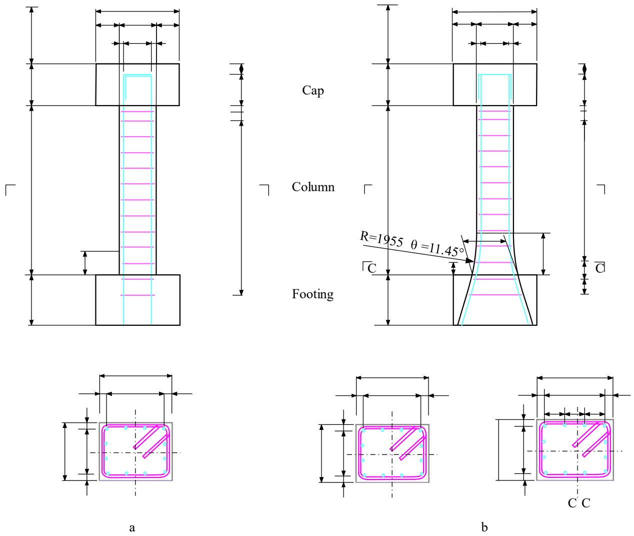


Fig.3: Schematic diagram of reinforcements (a) Type 1 (b) Type 2

Material model

## 3. Material model

### 3.1. Concrete

Total strain rotating crack model with parabolic behavior for compression and exponential softening for tensile was employed to simulate the behaviors of concrete, as the shown in the Fig.4.

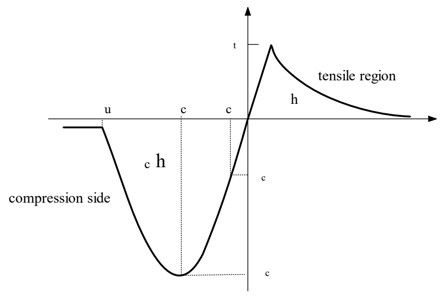


Fig.4: Behavior of concrete in tensile and compression

The compression curve was described by three characteristic strains corresponding to the maximum compressive strength $f_c$. The first one was the strain ($\alpha_{c/3}$) at which one-third of the maximum compressive strength is reached. The second one was $\alpha_c$ when the maximum compressive strength was reached. The last one was ultimate strain $\alpha_u$ in compression, which

**Keywords:** Improve toughness, RC pier, cyclic loading, FEM
Contact information: Kyushu University, 744 Motooka Nishiku, Fukuoka 819-0395, Japan, +81-928023371

meant the material was completely softened. the exponential law was adopted to reproduce the tensile softening response because it leaded to more localized crack and avoided large areas of diffuse cracking. The material parameters for concrete were summarized in Table.1.

Table 1: Parameters for concrete

| arameters | | Concrete |
|---|---|---|
| Young's modulus N mm | | |
| oisson's ratio | | . |
| Tensile behavior | Tensile curve | Exponential |
| | Tensile strength N mm | |
| | Compressive energy N mm | . |
| Compressive behavior | Compressive curve | arabolic |
| | Compressive behavior N mm | |
| | Compressive energy N mm | . |

## 3.2. Rebars

The stress-strain relationship for steel bars characterized by Dodd-Restrepo model based on the isotropic plasticity, as the Fig.5 shown. The curve was defined using elastic modulus $E$, yield strength $f_y$, Strain at end of yield plateau $\varepsilon_{su}$, breaking strength $f_u$, ultimate strain $\varepsilon_u$. The relevant material parameters used in the simulation for steel bar were summarized in Table.2. The bond-slip interface failure model is characterized by Shima bond-slip function, as the Fig.6 shown. Where τ was the bond stress M a , $f_{ck}$' was the compressive strength of concrete (MPa), $s$ was the amount of slip (mm) and D was the diameter of the reinforcement (mm). The material parameters for concrete were summarized in Table.3.

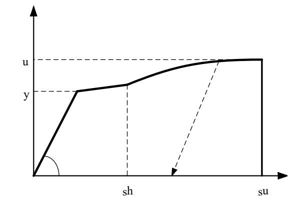


Fig.5: The relationship of stress-strain for rebars

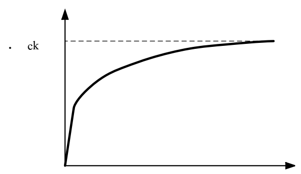


Fig.6: Bond-ship model

Table 2: Parameters for rebars

| arameters | Longitudinal rein orcement | | stirrup |
|---|---|---|---|
| Type | | | |
| Young's modulus N mm | | | |
| oisson's ratio | . | . | . |
| Yield stress N mm | | | |
| Strain at end o yield plateau | . | . | . |
| Ultimate strain | . | . | . |
| eak stress N mm | | | |

Table 3: Parameters for rebars

| arameters | Steel bar |
|---|---|
| ond slip inter ace ailure model | Shima bond slip |
| Normal sti ness modulus N mm | |
| Shear sti ness modulus N mm | |
| Compressive strength N mm | . |

## 4. Results and discussion

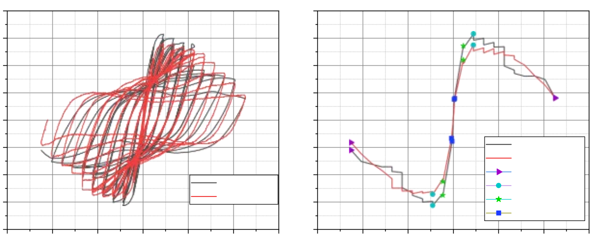

a b

Fig. 7: Comparison between simulation and experiment for type 1(a) Hysteretic curves for simulation and experiment (b) Skeleton curves for simulation and experiment

To verify the accuracy of finite model, the model was first employed to simulate, and the results of simulation were compared with experimental results according to the force-lateral displacement hysteretic curves, skeleton curves and the crack distribution for specimens. The Fig.7 and Fig.8 shows the comparison of hysteretic curves and skeleton curves between results of simulation and experiment. It can be seen the crack point, yield point, peak point, ultimate point and trend of curves predicted by the numerical simulation matches well with experimental results for type 1 and type 2.

It is deserved to mention that the rupture and buckling of rein orcements don't explicitly appear in the model. However, considering the hysteretic curves, skeleton curves and cracks distribution, it may be reasonable to deduce the other factors influenced on the toughness for the specimens by using the same material parameters.

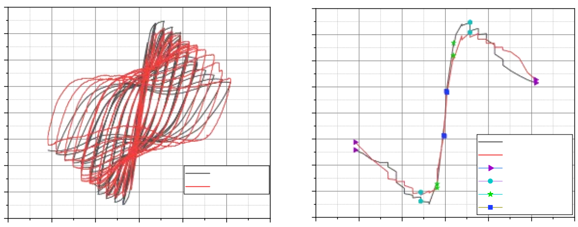

a b

Fig. 8 Comparison between simulation and experiment for type 2 (a) Hysteretic curves for simulation and experiment (b) Skeleton curves for simulation and experiment

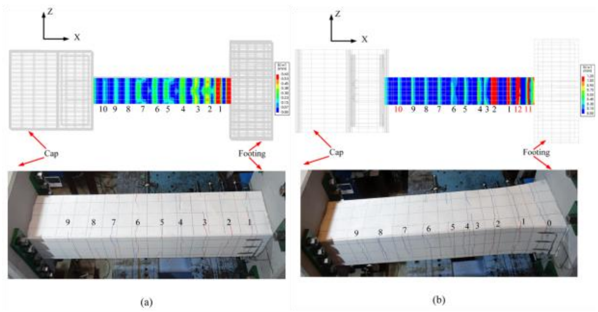


Fig. 9 Simulation and experiment Crack distribution

## 5. CONCLUSIONS

In this study, non-linear finite element method analyses were also carried out to investigate the usefulness of the proposed method by DIANA and validated against the experiment results. It is deserved to mention that the rupture and buckling o rein orcements don't explicitly appear in the model. However, considering the hysteretic curves, skeleton curves and cracks distribution, it may be reasonable to deduce the other factors influenced on the toughness for the specimens by using the same material parameters.

## REFERENCE

[1] D. Zhang, N. Li, Z.-X. Li, L. Xie, Experimental investigation and con- finement model of composite confined concrete using steel jacket and prestressed steel hoop, Construction and Building Materials 256 (2020) 119399.

[2] R. M. Faysal, M. M. H. Bhuiyan, K. Al Momin, T. Tafsirojjaman, Y. Liu, A review on the advances of the study on frp-concrete bond under hygrothermal exposure, Construction and Building Materials 363 (2023) 129818.

[3] S. Kim, Y. Jeong, M. Kwon, J. Kim, Ductile behavior of RC column reinforced with velcro seismic reinforcement system (vsrs), in: Structures, Vol. 44, Elsevier, 2022, pp. 796–808.

[4] T. Y. Yuen, J. Kuang, D. Y. Ho, Ductility design of rc columns. part 2: extent of critical zone and confinement reinforcement, HKIE Trans- actions 24 (1) (2017) 42